Appl. Phys. A (2016) 122:402
DOI 10.1007/s00339-016-9960-7

Applied Physics A
Materials Science & Processing

Glass-forming ability and rigidity percolation in SeTePb lone-pair semiconductors

Pankaj Sharma[1]

Received: 29 July 2015 / Accepted: 29 February 2016 / Published online: 15 March 2016
© Springer-Verlag Berlin Heidelberg 2016

Abstract Correlating the various physical parameters of known semiconductors and pointing the properties of new ones, a number of parameters have been employed recently with different levels of success. Taking this into account an attempt has been made to correlate the physical properties of Pb-doped Se–Te lone-pair semiconductors. The small band gap and large Bohr radius of lead (Pb) containing lone-pair semiconductors assist them with specific optical, electrical and thermal properties. The various physical parameters like number of constraints, lone pair of electron, heat of atomization, density, compactness, free volume percentage have been analyzed in terms of mean coordination number for $(Se_{90}Te_{10})_{100-x}Pb_x$ ($x = 0$, 4, 8, 12, 16, 20, 24). The band gap for the compositions has been determined theoretically, and the obtained results are very well explained in terms of cohesive energy, electronegativity and average single bond energy.

1 Introduction

Conventional oxide glasses have established general applications in our lives, e.g., in window glass, screens, container glass and electric bulbs to LCDs and optical fibers. Chalcogenides are glasses obtained by mixing the chalcogen elements sulfur, selenium and tellurium with themselves or with other elements in the periodic table. Since chalcogenide glasses have lone pair of electron and semiconducting nature, they are also termed as lone-pair semiconductors. Chalcogenide glasses are usually rugged and weakly bonded in comparison with oxide glasses. Chalcogenides have created deep interest in the technological communities as materials beautifying interesting physics and offering large potential for applications in the field of mid-infrared lasers [1], optical fibers [2], ultra-fast photonic processing devices operated in IR region [3, 4], sensors [5], thermal imaging [6], etc. Chalcogenide glasses are long familiar for their prominent non-resonant, third-order nonlinearity and extraordinary optical transmittance in near-to-far-IR region [7–10].

Among the several chalcogenide glassy systems, Se–Te system is preferred on account of its higher photosensitivity, better hardness, high crystallization temperature and shorter aging effects in comparison with pure selenium [11, 12]. The addition of a third element (like Sb, Sn, In, Ag, Ge and Bi) to Se–Te system has prominent effect on its structural, physical, optical, electronic and thermal properties [12–18]. Moreover, the introduction of the third element enlarges the glass-forming area, and it may produce compositional disorder in Se–Te glass. The small band gap and large Bohr radius of Pb may facilitate Se–Te system with unique optical, electrical and thermal properties. Moreover, Pb chalcogenides have become good candidates for the potential applications in solar cells, photodetectors, field-effect transistor and as sensitive membrane materials for the development of conventional chemical sensors selective to metal ions in liquid media as well as biological imaging [19–21]. The growth of laser technology has introduced new applications for IV–VI group materials. The laser diodes based on lead chalcogenides and their solid solutions are significant sources for the tunable emissions in the mid-IR region. Therefore, in the present work, Pb has been

✉ Pankaj Sharma
pankaj.sharma@juit.ac.in; pks_phy@yahoo.co.in

[1] Department of Physics and Materials Science, Jaypee University of Information Technology, Waknaghat, Solan, H.P. 173234, India

Table 1 Values of density, coordination number, electronegativities, band gap, heat of atomization ($\bar{H}_S$) and atomic volume of Se, Te and Pb used

	Te	Se	Pb
Density (g cm^{-3})	6.24	4.819	11.34
Coordination number	2	2	4
Electronegativity	2.10	2.55	2.33
Band gap (eV)	0.335	1.95	0
Heat of atomization (kJ/mol)	196.7	227.1	195.2
Atomic weight	127.6	78.96	207.2

Elemental composition of $(Se_{90}Te_{10})_{100-x}Pb_x$ (x = 0, 4, 8, 12, 16, 20, 24) bulk glasses

Elemental composition (at.%)			
Sample	Se	Te	Pb
$x = 0$	89.78	10.22	0
$x = 4$	86.21	9.82	3.97
$x = 8$	82.82	9.22	7.96
$x = 12$	79.15	8.78	12.07
$x = 16$	75.67	8.36	15.97
$x = 20$	72.10	7.96	19.94
$x = 24$	68.38	7.54	24.08

chosen as third element for the addition to Se–Te glassy system. Glasses with ~10 at.% Te contents have been reported to have the greatest resistance to crystallization [22]. Hence, $Se_{90}Te_{10}$ glassy system has been chosen for the investigation and is subsequently replaced by Pb.

In the present work, $(Se_{90}Te_{10})_{100-x}Pb_x$ (x = 0, 4, 8, 12, 16, 20, 24) alloys have been synthesized via melt-quench technique and studied for the glass-forming ability, free volume percentage, mean coordination number, number of constraints, number of lone-pair electron, heat of atomization, cohesive energy, mean bond energy and glass transition temperature. A correlation has been drawn between the mean coordination number and various other investigated physical parameters.

2 Experimental details

Alloys of $(Se_{90}Te_{10})_{100-x}Pb_x$ (x = 0, 4, 8, 12, 16, 20, 24) have been synthesized using melt-quenching technique. Melt quenching substantially enhances the glassy domain due to the faster quenching rate. Glasses with wide variety of compositions are possible. Moreover, melt-quenching technique does not require stoichiometry. High-purity elements Se, Te and Pb in the appropriate weight proportions have been vacuum sealed (~10^{-4} Pa) in quartz ampoules and heated up to 773 K in a rocking furnace at a heating rate of 3–4 K/min and kept at the highest temperature for 8 h. The ampoules have been rocked many times at short intervals at the highest temperature. The quenching has been done in ice-cold water immediately after taking out the ampoules from the furnace. The bulk samples have been used to measure the density by Archimedes (buoyancy) method. The double-distilled water has been used as a reference liquid at 293 K. The densities of samples have been calculated using the relation: $\rho = \{w_a/(w_a - w_l)\} \times \rho_l$, where w_a and w_l are the weights of samples in air and in the reference liquid, respectively, while ρ_l (=1 g cm^{-3} at 20 °C) is the density of the liquid. The densities have been measured five times, and the average values are reported. The bulk alloys have been characterized by X-ray diffraction technique. Bulk samples have been characterized using energy-dispersive X-ray spectroscopy (EDAX) (Zeiss EVO 40 EP with EDAX attachment operated at 20 kV) for the analysis of compositions (Table 1). No prominent peak has been observed in the spectra which confirm the amorphous nature of samples (Fig. 1).

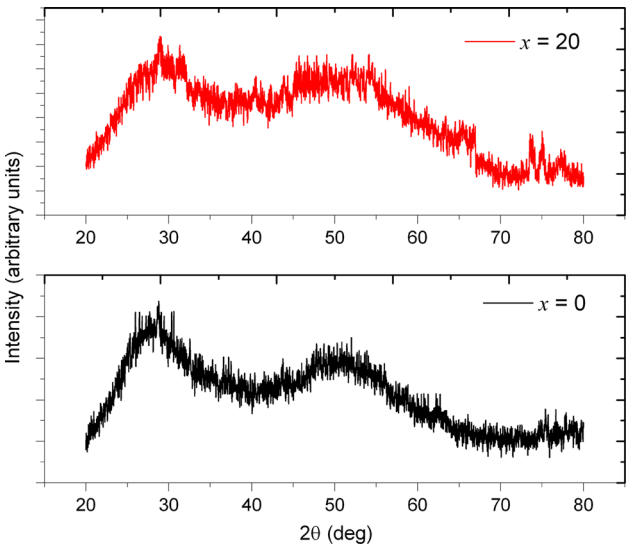

Fig. 1 X-ray diffraction spectra for $(Se_{90}Te_{10})_{100-x}Pb_x$ (x = 0, 20) as reference

3 Results and discussion

3.1 Mean coordination number <r> and network topology

On the atomic scale, the structure of chalcogenide glasses is most satisfactorily depicted using the continuous random network model, in which means coordination number

Table 2 Some physical parameters as a function of Pb content for $(Se_{90}Te_{10})_{100-x}Pb_x$ system

x	$<r>$	N_α	N_β	N_c	$<r_{eff}>$	ρ (g cm^{-3})	δ	V_m (cm^{-3})	FVP
0	2.00	1.00	1.00	2.0	2.00	4.944	−0.0096	16.95	0.962
4	2.08	1.04	1.16	2.2	2.08	5.121	−0.0278	17.33	2.778
8	2.16	1.08	1.32	2.4	2.16	5.384	−0.0283	17.40	2.829
12	2.24	1.12	1.48	2.6	2.24	5.652	−0.0276	17.45	2.757
16	2.32	1.16	1.64	2.8	2.32	5.921	−0.0265	17.49	2.645
20	2.40	1.20	1.80	3.0	2.40	6.288	−0.0097	17.25	0.970
24	2.48	1.24	1.96	3.2	2.48	6.407	−0.0315	17.70	3.152

($<r>$) is an important parameter [3]. The mean coordination number (i.e., the sum of the products of the individual copiousness times the valency of the constituent atoms) for $(Se_{90}Te_{10})_{100-x}Pb_x$ ($x = 0, 4, 8, 12, 16, 20, 24$) system has been calculated using the equation: $<r> = (\alpha N_{Se} + \beta N_{Te} + \gamma N_{Pb})/100$, where α, β and γ are the atomic % of Se, Te and Pb, respectively, and N_{Se}, N_{Te} and N_{Pb} are their respective coordination numbers (Table 1). Twofold Se chains or Se rings have been first cross-linked by Te atoms and then by fourfold Pb atoms. The addition of fourfold-coordinated atoms makes the three-dimensional network and hence increases the mean coordination number. The calculated values of mean coordination number have been given in Table 2. The increase in mean coordination number may raise the network rigidity, strength and density of the compositions and will also affect other physical parameters. Mean coordination number gives well-defined nearest neighbors. The relationships between the $<r>$, network topology and the various other physical properties of chalcogenide glasses have been investigated by numerous researchers [13, 17, 23–25].

Mean coordination number in the ternary system $(Se_{90}Te_{10})_{100-x}Pb_x$ is suitable for testing the validity of topological concepts [23, 24] due to its large glass-forming domain. The values of $<r>$ lie in the range $2.0 \leq <r> \leq 2.48$ (Table 2). In covalent solids, there are two types of near-neighbor bonding forces: bond stretching (N_α) and bond bending (N_β). These interatomic valence forces constrain mechanically the covalent bonded glassy network. The number of constraints has been determined by considering the stability of a network of rods connected with pivot joints. Bond-stretching constraints appear from the radial force, and bond-bending constraints come due to angular forces. The average number of constraints per atom arising from bond bending has been estimated by using: $N_\beta = 2<r> - 3$, and the average number of constraints per atom arising from bond stretching have been computed from $N_\alpha = <r>/2$, for the atomic species having mean coordination number ($<r>$). The average number of total constraints (N_c) has been calculated just by adding the average constraints arising from bond stretching and bond bending. These mechanical constraints (N_c) are coupled with atomic bonding and effective coordination number $<r_{eff}>$. For different compositions of $(Se_{90}Te_{10})_{100-x}Pb_x$ system, the effective coordination number $<r_{eff}>$ can be calculated from the relation: $<r_{eff}> = (2/5) \times (N_c + 3)$. The calculated values of N_α, N_β, N_c and $<r_{eff}>$ have been listed in Table 2. According to Thorpe [24], the system should contain floppy (mean coordination number <2.4) and rigid regions (mean coordination number >2.4) in the range of the glass-forming compositions. The best consideration for glass formation according to Phillips and Thorpe [25] occurs when N_c is equal to the degree of freedom (N_d), i.e., when $N_c = N_d = 3$ which corresponds to $<r> = 2.4$ (here for $x = 20$ at.%).

The analysis of constraints for a network helps us to uncover various substructures and mechanical softening of covalently bonded networks. Network with mean coordination number <2.4 is polymeric glasses (or in floppy mode) where the rigid regions are unconnected or isolated. With an increase in $<r>$ value, the network goes through a transition at $<r> = 2.4$; here, the networks are considered to be optimally coordinated and at a mechanically critical point. With further increase in $<r>$, the rigidity percolates and the glass transforms to a rigid structure. Networks for $<r>$ >2.4 are in rigid mode or over-coordinated. In present case, for $x > 20$ at.% there is rigidity percolation and a transition from two-dimensional structural network to three-dimensional structural network occurs.

3.2 Density, molar volume, free volume percentage and compactness

The density has been observed to increase linearly with the addition of Pb content (Table 2). This can simply be explained on the basis that low-density constituents are replaced by high-density Pb element (Table 1). Further, the increase in density can be explained on the basis of chemical bond formation, since heteropolar Pb–Se has large bond formation probability as compared to homopolar Se–Se bonds, which results in an increase in number of bonds per unit volume and increase in average cross-linking density with Pb addition.

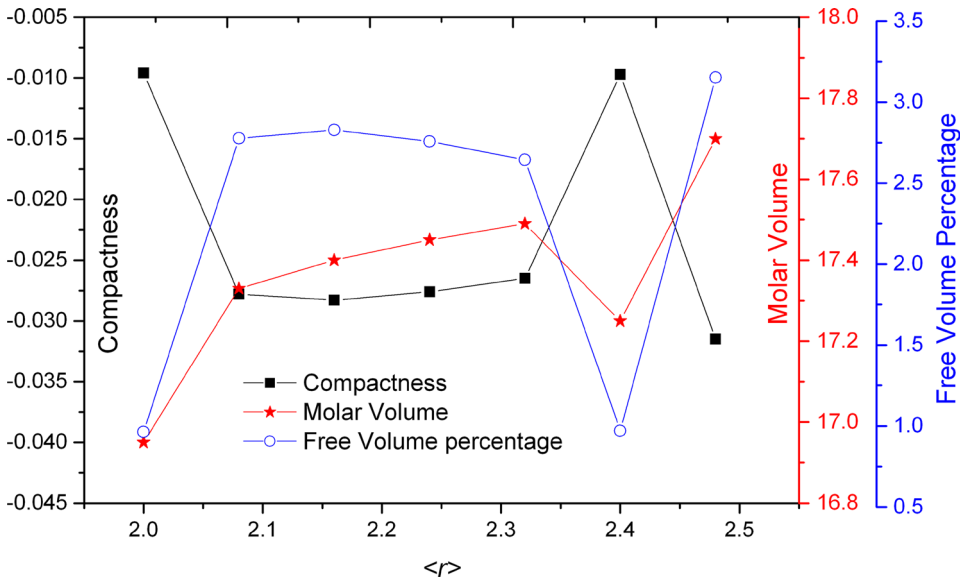

Fig. 2 Variation of compactness, molar volume and free volume percentage with mean coordination number <*r*> for $(Se_{90}Te_{10})_{100-x}Pb_x$ system

Molar volume (V_m) has been calculated from density of investigated samples using the relation: $V_m = (\sum x_i m_i)/\rho$, where m_i is molecular weight of ith element and x_i is the atomic percentage of same element. The molar volume increases linearly with the addition of Pb content for <*r*> = 2.0 (i.e., at $x = 0$) to <*r*> = 2.4 (i.e., at $x = 20$), and then, interestingly it decreases for mean coordination number more than 2.4. This abrupt behavior may be explained on the basis of rigidity percolation.

The free volume percentage (FVP) for the samples has been calculated using the relation: FVP = $\{(V_m - V_T)/V_m\} \times 100$, where V_T is the theoretically obtained molar volume. The theoretical molar volume has been calculated for various samples using the additive formula given elsewhere [26]. The values of FVP are listed in Table 2. The FVP has been found to be maximum for <*r*> = 2.4. The changes in FVP are due to the modification in the composition structure that has been induced by the variation in interatomic spacing, which could be assigned to the change in the number of bonds per unit volume of the glassy network.

The compactness of the compositions has been calculated using the relation given elsewhere [26]. Figure 2 shows the variation of compactness with the mean connectedness for the compositions under investigation. The compactness has been found to be maximum for <*r*> = 2.4, whereas the molar volume and FVP have minima at <*r*> = 2.4. This can be explained on the basis of rigidity percolation theory [25]. The optimum mechanical stability of the glass, with <*r*> = 2.4 where the transformation from a floppy to a rigid network takes place, is linked with the maximum compactness of the glassy structure [27]. Therefore, the free volume percentage in glass for <*r*> = 2.4 is minimum.

3.3 Heat of atomization, average single bond energy, theoretical band gap and cohesive energy

The general applicability of average heats of atomization lies in the reflection of the relative bond strength. The properties of semiconducting chalcogenide compounds can be correlated with the average heat of atomization. The lone-pair electron makes the top of valence band, and the antibonding band makes the bottom of conduction band in chalcogenide glasses [28]. In case of chalcogenide glasses, the heat of formation imparts very little for the average heat of atomization because the electronegativities of the constituent elements, i.e., Se, Te and Pb, are very similar, and in most of the cases of chalcogenide glasses, the heat of formation is unknown. For the system under investigation, the heat of atomization has been calculated using the relation given elsewhere [29]. The values of heat of atomization for Se, Te and Pb elements are given in Table 1. The calculated average heat of atomization $\bar{H}_S$ in kJ/mol and average single bond energy $(\bar{H}_S/\langle r \rangle)$ are given in Table 3, where <*r*> is the mean coordination number. It is clear from Table 3 that the average heat of atomization decreases with an increase in Pb content. A similar behavior for the average single bond energy $(\bar{H}_S/\langle r \rangle)$ which is a measure of cohesive energy has been observed with an increase in Pb content. This decrease in the average single bond energy with the increase in Pb content may cause the decrease in energy gap (calculated later). An easy view can be seen in Fig. 3 showing the variation of energy gap along with average single bond energy with Pb content.

The energy gap (E_g) for $(Se_{90}Te_{10})_{100-x}Pb_x$ compositions has also been computed theoretically using the relation given elsewhere [30]. It has been found that the energy

Table 3 Values of heat of atomization ($\bar{H}_S$), average single bond energy ($\bar{H}_S/\langle r\rangle$), electronegativity ($\chi$), band gap ($E_g$), possible percentage distribution of chemical bonds and cohesive energy (CE) for $(Se_{90}Te_{10})_{100-x}Pb_x$ system

x	$\bar{H}_S$	$\bar{H}_S/\langle r\rangle$	E_g (eV)	χ	Possible percentage distribution of chemical bonds			CE (kJ/mol)
					Pb–Se	Se–Te	Se–Se	
0	223.970	111.985	1.753	2.50	0	11.11	88.89	184.18
4	222.819	107.125	1.677	2.494	9.26	11.11	79.63	179.75
8	221.668	102.624	1.601	2.487	19.32	11.11	69.57	174.93
12	220.518	98.445	1.526	2.480	30.30	11.11	58.59	169.68
16	219.367	94.555	1.452	2.473	42.33	11.11	46.56	163.92
20	218.216	90.923	1.378	2.466	55.56	11.11	33.33	157.59
24	217.065	87.526	1.305	2.459	70.18	11.11	18.71	150.59

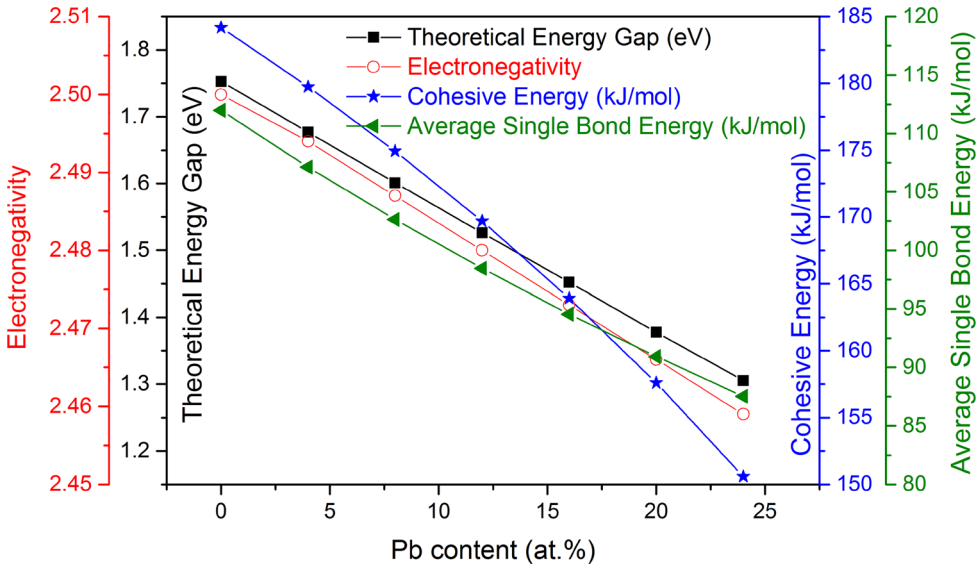

Fig. 3 Variation of some physical parameters with Pb content for $(Se_{90}Te_{10})_{100-x}Pb_x$ system

gap decreases with the addition of Pb to Se–Te system. The decrease in energy gap can be explained via the decrease in average single bond energy (Table 3). This decrease can also be correlated with decrease in electronegativity of the system with increasing Pb content (Table 3). The electronegativity values for various compositions have been calculated using Sanderson's method [31]. Further, the decrease in energy gap has been correlated with the decrease in overall bond energy of the system. According to chemical bond approach [32], heteropolar bonds form more easily in comparison with homopolar bonds. Considering this the bond energy of the possible bonds has been calculated using Pauling's relation: $E_{A-B} = (E_{A-A} \times E_{B-B})^{0.5} + 30(\chi_A - \chi_B)^2$, where E_{A-A} and E_{B-B} are the bond energies of the homopolar bonds and χ_A and χ_B are the electronegativities of the atoms involved (Table 1). The bond energies of Pb–Se bonds (bond energy = 136.25 kJ/mol) which are supposed to form at the expense of Se–Se bonds (bond energy = 184.096 kJ/mol) may lower the overall energy of the system and hence decrease the energy gap.

According to chemical bond approach [32], heteropolar bonds form more easily in comparison with homopolar bonds. The different types of bonds possible in the present system are Se–Se (184.096 kJ/mol), Te–Te (138.072 kJ/mol), Pb–Pb (92.048 kJ/mol), Se–Te (184.85 kJ/mol), Pb–Se (136.25 kJ/mol) and Te–Pb (119.38 kJ/mol). These bonds are formed in the sequence of their decreasing bond energy. This is equivalent to assuming the maximum possible amount of chemical ordering. Consequently, Se–Te bonds will form first followed by Pb–Se, still some of the Se will remain, and hence, in last homopolar Se–Se bonds will form. The possible chemical bond distribution is given in Table 3.

Cohesive energy is the amount of energy (normalized per atom, per electron, etc.) that a system acquires by being in a solid phase as compared to the phase in which atoms are so far apart that their electronic wave functions do not

overlap. Cohesive energy of a solid is therefore the energy required to break all the bonds associated with its constituent atoms. Further, the cohesive energy has been calculated by summing the bond energies over all expected bonds for the compositions under investigation. It has been observed that the cohesive energy decreases with an increase in Pb content (Table 3), as cohesive energy is the stabilization energy of an infinitely large cluster of material per atom, so, can be correlated with energy gap of material. Therefore, the decrease in energy gap can also be explained with the decrease in cohesive energy.

3.4 Lone-pair electron favors glass-forming ability

Non-bonding pair of electrons that are lying in valence band is termed as lone pair of electron (L). Since chalcogenide glasses possess lone-pair electron, they are also named as lone-pair glassy semiconductors. The presence of lone-pair electron removes the strain force caused by the formation of amorphous materials. The chemical bonds formed with these non-bonding electrons have the quality of flexibility. Thus, large number of lone-pair electron will favor the glass formation by reducing the strain energy of the system. The number of lone-pair electrons in system can be calculated from the difference of all the valence electrons of the system and the mean coordination number. The values of lone-pair electron are tabulated in Table 4. The number of lone-pair electron decreases with the addition of Pb to Se–Te system. This is caused by the interaction between the Pb ions and the lone-pair electrons of bridging Se atoms. The interaction diminishes the role of lone-pair electrons in the glass formation. To check the ability of glass formation in chalcogenides, a simple criterion has been proposed [33]. The criterion proposes that for a binary system $L > 2.6$ and for ternary system $L > 1$. In present analysis, it is seen that $L > 3$ for all compositions. Thence, the compositions under investigation may be considered as good glass formers.

Table 4 Values of lone-pair electron (L), deviation from stoichiometry (R), mean bond energy ($<E>$) and glass transition temperature (T_g) for $(Se_{90}Te_{10})_{100-x}Pb_x$ system

x	L	R	$<E>$ (eV)	T_g (K)
0	4	–	1.919	316.98
4	3.84	10.99	1.865	300.22
8	3.68	5.36	1.831	289.58
12	3.52	3.48	1.815	284.41
16	3.36	2.53	1.814	284.13
20	3.2	1.96	1.827	288.25
24	3.04	1.58	1.853	296.36

3.5 Deviation from stoichiometry and prediction of glass transition temperature

The ratio of covalent bonding assumptions of chalcogen atom to that of non-chalcogen atom led to measure the deviation from stoichiometry (also known as parameter R) in the compositions under investigations. If the value of R comes to be more than unity for a composition, then the composition is considered as chalcogen rich, and for value less than unity composition is considered as chalcogen poor. The calculated values of R have been listed in Table 4. It has been found that $R > 1$ for all the investigated compositions, making sure that our system is chalcogen rich.

Chalcogenide glasses have generally covalent bonding as van der Waals interactions between layers are not strong in comparison with intra-layer interaction (i.e., covalent bonding). At glass transition temperature (T_g), glassy network is macroscopically mobile because of clear-cut decrease in the viscosity. The distinct decrease in the viscosity above the glass transition temperature is anticipated to be due to crumbling of glassy network up to some degree. Tichy and Ticha [34, 35] proposed that the bond energy for each bond, i.e., mean bond energy ($<E>$), should be taken into account for total network. In their proposal, a covalent bond approach in chalcogenide glasses has been considered, which produces a good correlation between glass transition temperature and the mean bond energy. Thus, this model comprises the factors of mean coordination number and the mean bond energy. Tichy and Ticha [34, 35] examined 186 binary and ternary chalcogenide glasses with T_g ranging from 320 to 760 K and gave an empirical relation: $T_g = 311[<E> - 0.9]$. The mean bond energy ($<E>$) of the system has been calculated using the relation: $<E> = E_C + E_{rm}$, where E_c is the overall contribution toward bond energy arising from strong heteropolar bonds and E_{rm} is the contribution arising from weaker bonds that remain after the number of strong heteropolar bonds will become maximum, i.e., average bond energy per atom of the 'remaining matrix.' The calculated values of the mean bond energy are listed in Table 4. This is clear from mean bond energy data that when Pb content increases, the mean bond energy of the system decreases. These $<E>$ data have been used for the prediction of glass transition temperature. The glass transition temperature has been plotted in Fig. 4 with mean coordination number. The glass transition temperature of the system under consideration shows a decrease with the increase in the Pb content. Heteropolar Pb–Se bonds (136.25 kJ/mol) are supposed to form at the cost of Se–Se homopolar bonds (184.096 kJ/mol). This will decrease the overall bond energy of the system and hence the glass transition temperature.

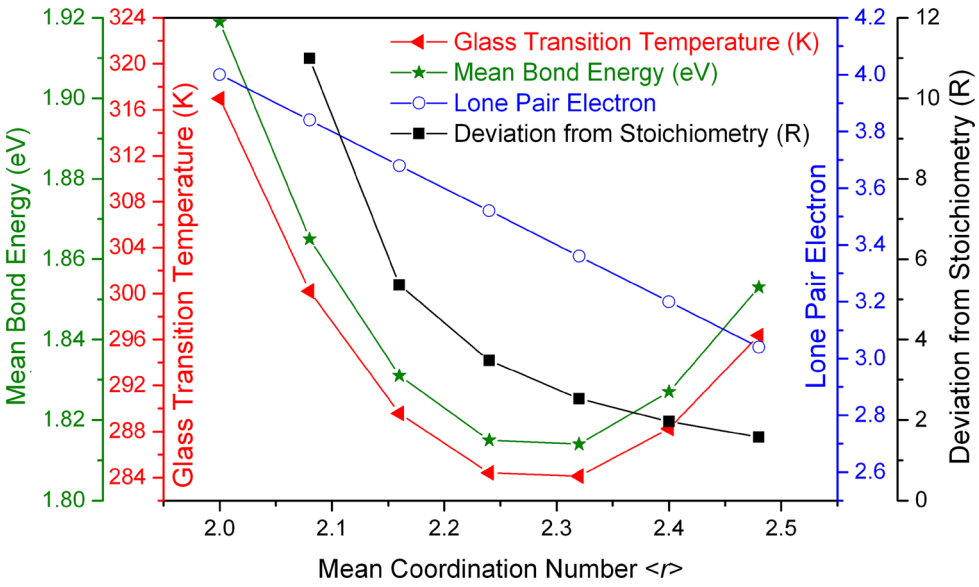

Fig. 4 Plot showing the variation of some physical parameters with mean coordination number for $(Se_{90}Te_{10})_{100-x}Pb_x$ system

4 Conclusions

Glass-forming ability and the implications of compositions on the constraints for $(Se_{90}Te_{10})_{100-x}Pb_x$ ($x = 0$, 4, 8, 12, 16, 20, 24) have been investigated, and thereby, the system has been speculated for percolation with mean coordination number. It has been observed that for $x > 20$ at.% there is rigidity percolation and a transition from two-dimensional structural network to three-dimensional structural network occurs. The compactness has been found to be maximum for $<r> = 2.4$, whereas the molar volume and FVP have minima at $<r> = 2.4$. The density has been observed to increase linearly with the addition of Pb content. The number of lone-pair electron decreases with the addition of Pb to Se–Te system, but still found to be sufficient for helping in glass formation. The energy gap decreases with the addition of Pb to Se–Te system, which has been confirmed by the decrease in average single bond energy as well as the decrease in electronegativity of the system. The glass transition temperature has been observed to decrease with increasing Pb content. The cognitive content of next research is to compound the understanding of SeTePb lone-pair semiconductors using various experimental characterizations.

Acknowledgments The author would like to thank Dr. Vineet Sharma, JUIT Waknaghat for fruitful discussion during this work.

References

1. M. Zhang, A. Yang, Y. Peng, B. Zhang, H. Ren, W. Guo, Y. Yang, C. Zhai, Y. Wang, Z. Yang, D. Tang, Mater. Res. Bull. **70**, 55–59 (2015)
2. A. Galstyan, S.H. Messaddeq, V. Fortin, I. Skripachev, R. Vallée, T. Galstian, Y. Messaddeq, Opt. Mater. (2015). doi:10.1016/j.optmat.2015.06.032
3. B.J. Eggleton, B. Luther-Davies, K. Richardson, Nat. Photonics **5**, 141–148 (2011)
4. J. Hu, J. Meyer, K. Richardson, L. Shah, Opt. Mater. Exp. **3**(9), 1571–1575 (2013)
5. Y. Ermolenko, D. Kalyagin, I. Alekseev, E. Bychkov, V. Kolodnikov, N. Melnikova, I. Murin, Y. Mourzina, Y. Vlasov, Sens. Actuators B Chem. **207**, 940–944 (2015)
6. A.L. Zelazny, K.F. Walsh, J.P. Deegan, B. Bundschuh, E.K. Patton, in *Proceedings of the SPIE 9451, Infrared Technology and Applications XLI*, 94511M1-11
7. P. Sharma, S.C. Katyal, J. Appl. Phys. **107**, 113527 (2010)
8. K. Ogusu, J. Yamasaki, S. Maeda, M. Kitao, M. Minakata, Opt. Lett. **29**, 265–267 (2004)
9. J.T. Gopinath, M. Soljai, E.P. Ippen, V.N. Fuflyigin, W.A. King, M. Shurgalin, J. Appl. Phys. **96**, 6931–6933 (2004)
10. P. Sharma, S.C. Katyal, J. NonCryst. Solids **354**, 3836–3839 (2008)
11. B. Bureau, C. Boussard-Pledel, P. Lucas, X. Zhang, J. Lucas, Molecules **14**, 4337–4350 (2009)
12. K.A. Aly, F.M. Abdel Rahim, A. Dahshan, J. Alloys Compd. **593**, 283–289 (2014)
13. S. Saraswat, S.D. Sharma, Glass Phys. Chem. **41**, 402–409 (2015)
14. P. Yadav, A. Sharma, J. Electron. Mater. **44**, 916–921 (2015)
15. R. Kumar, P. Sharma, V.S. Rangra, J. Therm. Anal. Calorim. **109**, 177–181 (2011)
16. V.K. Saraswat, V. Kishore, N.S. Deepika, N.S. Saxena, T.P. Sharma, L.I. Singh, P.K. Saraswat, Chalcogenide Lett. **5**, 95–103 (2008)
17. M.A. Abdel-Rahim, M.M. Hafiz, A.Z. Mahmoud, Appl. Phys. A **118**, 981–988 (2015)
18. N. Sharma, S. Sharda, D. Sharma, V. Sharma, P.B. Barman, S.C. Katyal, P. Sharma, S.K. Hazra, Electron. Mater. Lett. **9**, 629–633 (2013)
19. R.D. Schaller, V.I. Klimov, Phys. Rev. Lett. **92**, 186601 (2004)
20. R.J. Ellingson, M.C. Beard, J.C. Johnson, P. Yu, O.I. Micic, A.J. Nozik, A. Shabaev, A.L. Efros, Nano Lett. **5**, 865–871 (2005)
21. S.A. Mcdonald, G. Konstantatos, S. Zhang, P.W. Cyr, E.J.D. Klem, L. Levina, E.H. Sargent, Nat. Mater. **4**, 138–142 (2005)

22. S.O. Kasap, T. Wagner, V. Aiyah, O. Krylouk, A. Bekirov, J. Mater. Sci. **34**, 3779–3787 (1999)
23. J.C. Phillips, J. NonCryst. Solids **34**, 153–181 (1979)
24. M.F. Thorpe, J. NonCryst. Solids **57**, 355–370 (1983)
25. J.C. Phillips, M. Thorpe, Solid State Commun. **53**, 699–702 (1985)
26. S.S. Fouad, M.S. El-Bana, P. Sharma, V. Sharma, Appl. Phys. A **120**, 137–143 (2015)
27. G. Saffarini, J. Matthiesen, R. Blachnik, Phys. B **305**, 293–297 (2001)
28. M. Kastner, Phys. Rev. Lett. **28**, 355–357 (1972)
29. P. Sharma, S.C. Katyal, J. Optoelectron. Adv. Mater. **9**, 1994–1999 (2007)
30. A. Dahshan, K.A. Aly, Philos. Mag. **88**, 361–372 (2008)
31. R.T. Sanderson, J. Chem. Edu. **65**, 112–118 (1988)
32. J. Bicerano, S.R. Ovshinsky, J. NonCryst. Solids **75**, 169–175 (1985)
33. L. Zhenhua, J. NonCryst. Solids **127**, 298–305 (1991)
34. L. Tichy, H. Ticha, J. NonCryst. Solids **189**, 141–146 (1995)
35. L. Tichy, H. Ticha, Mater. Lett. **21**, 313–319 (1994)